AFRL-PR-WP-TP-2006-267

CAVITY-BASED INJECTOR MIXING EXPERIMENTS FOR SUPERSONIC COMBUSTORS WITH IMPLICATIONS ON IGNITER PLACEMENT (POSTPRINT)

Lance S. Jacobsen, Campbell D. Carter, and Andrew C. Dwenger

OCTOBER 2006

Approved for public release; distribution is unlimited.

STINFO COPY

PROPULSION DIRECTORATE
AIR FORCE MATERIEL COMMAND
AIR FORCE RESEARCH LABORATORY
WRIGHT-PATTERSON AIR FORCE BASE, OH 45433-7251

REPORT DOCUMENTATION PAGE

Form Approved
OMB No. 0704-0188

1. REPORT DATE *(DD-MM-YY)*	2. REPORT TYPE	3. DATES COVERED *(From - To)*
October 2006	Conference Paper Postprint	N/A

4. TITLE AND SUBTITLE
CAVITY-BASED INJECTOR MIXING EXPERIMENTS FOR SUPERSONIC COMBUSTORS WITH IMPLICATIONS ON IGNITER PLACEMENT (POSTPRINT)

5a. CONTRACT NUMBER
In-house

5b. GRANT NUMBER

5c. PROGRAM ELEMENT NUMBER
61102F

6. AUTHOR(S)
Lance S. Jacobsen and Andrew C. Dwenger (GoHYPERSONIC Inc.)
Campbell D. Carter (AFRL/PRAS)

5d. PROJECT NUMBER
2308

5e. TASK NUMBER
AI

5f. WORK UNIT NUMBER
00

7. PERFORMING ORGANIZATION NAME(S) AND ADDRESS(ES)
GoHYPERSONIC Inc.
714 Monument Ave., Suite 201
Dayton, OH 45402

Propulsion Sciences Branch (AFRL/PRAS)
Aerospace Propulsion Division
Propulsion Directorate
Air Force Research Laboratory, Air Force Materiel Command
Wright-Patterson AFB, OH 45433-7251

8. PERFORMING ORGANIZATION REPORT NUMBER
AFRL-PR-WP-TP-2006-267

9. SPONSORING/MONITORING AGENCY NAME(S) AND ADDRESS(ES)
Propulsion Directorate
Air Force Research Laboratory
Air Force Materiel Command
Wright-Patterson AFB, OH 45433-7251

10. SPONSORING/MONITORING AGENCY ACRONYM(S)
AFRL-PR-WP

11. SPONSORING/MONITORING AGENCY REPORT NUMBER(S)
AFRL-PR-WP-TP-2006-267

12. DISTRIBUTION/AVAILABILITY STATEMENT
Approved for public release; distribution is unlimited.

13. SUPPLEMENTARY NOTES
Conference paper published in the Proceedings of the 2006 42nd AIAA/ASME/SAE/ASEE Joint Propulsion Conference and Exhibit, published by AIAA.

 PAO case number: AFRL/WS 06-1588; Date cleared: 22 June 2006. Paper contains color.

14. ABSTRACT
Mixing experiments using simultaneous acetone and NO PLIF were performed in the AFRL/PRA Test-cell 19 supersonic wind tunnel. These experiments investigated the influence of simulated plasma-torch placement in an injector-cavity configuration exposed to a supersonic crossflow. Both the simulated plasma torch and fuel injector holes injected room temperature air, respectively seeded with acetone and nitric oxide (NO). Experiments at the streamwise centerline of the rectangular wind tunnel investigated the differences between an aero-ramp and a single 15-degree downstream-angled injector in coupling to the recirculating flow in a downstream cavity. The influence of wall effects were investigated with a similar single-hole injector placed 3.5 injector diameters from the sidewall of the rectangular duct. Simulated plasma torch holes were tested up and downstream of the injectors, all upstream of the cavity. Tests took take place in a uniform Mach-2 crossflow; the respective tunnel total pressure and temperature were 1.7 atmospheres and 530 K.

15. SUBJECT TERMS

16. SECURITY CLASSIFICATION OF:			17. LIMITATION OF ABSTRACT:	18. NUMBER OF PAGES	19a. NAME OF RESPONSIBLE PERSON (Monitor)
a. REPORT	b. ABSTRACT	c. THIS PAGE			Campbell D. Carter
Unclassified	Unclassified	Unclassified	SAR	20	19b. TELEPHONE NUMBER *(Include Area Code)* N/A

Standard Form 298 (Rev. 8-98)
Prescribed by ANSI Std. Z39-18

42nd AIAA/ASME/SAE/ASEE Joint Propulsion Conference & Exhibit
9 - 12 July 2006, Sacramento, California

AIAA 2006-5268

Cavity-Based Injector Mixing Experiments for Supersonic Combustors with Implications on Igniter Placement

Lance S. Jacobsen*,
GoHYPERSONIC Inc., Dayton, OH

Campbell D. Carter†,
Air Force Research Laboratory, WPAFB, OH

and

Andrew C. Dwenger‡
GoHYPERSONIC Inc., Dayton, OH

Mixing experiments using simultaneous acetone and NO PLIF were performed in the AFRL/PRA Test-cell 19 supersonic wind tunnel. These experiments investigated the influence of simulated plasma-torch placement in an injector-cavity configuration exposed to a supersonic crossflow. Both the simulated plasma torch and fuel injector holes injected room temperature air, respectively seeded with acetone and nitric oxide (NO). Experiments at the streamwise centerline of the rectangular wind tunnel investigated the differences between an aero-ramp and a single 15-degree downstream-angled injector in coupling to the recirculating flow in a downstream cavity. The influence of wall effects were investigated with a similar single-hole injector placed 3.5 injector diameters from the sidewall of the rectangular duct. Simulated plasma torch holes were tested up and downstream of the injectors, all upstream of the cavity. Tests took take place in a uniform Mach-2 crossflow, and in a shock train generated by duct backpressure. The tunnel total pressure and total temperature were 1.7 atmospheres and 530 K. Results from the experiments demonstrated the difference in coupling of the simulated plasma torch plumes with the two types of injectors. Without backpressure only small differences were shown between the injector near the sidewall and the one on centerline. In the region investigated, the aero-ramp mixed faster than the 15-degree injector as inferred by NO PLIF maximum intensity ratio and relative size of the jet plumes. Further, the close proximity of the 15-degree injector to the corner was found to decrease the near-field mixing of the injector as compared to the centerline results.

Introduction

CAVITY-coupled scramjet ignition concepts have been under investigation at the Air Force Research Laboratory, AFRL, for several years[1,2]. In general, these concepts revolve around igniting the main fuel flow of a scramjet through the use of a cavity pilot flame. Coupling of the cavity flame to flush wall and in-stream injectors to allow propagation and pressure rise – leading to ignition – has proven difficult at low flight Mach numbers and dynamic pressures. This has motivated research at the AFRL on alternate ignition strategies for lighting this injector -cavity coupled combustor concept. Concepts involving plasmas and thermal ignition devices have been under development in order to address this problem[2,3,4]. The general strategy behind the use of these devices as igniters involves the utilization of jet momentum (from the devices) and proper placement to bridge the gap between the cavity flame and the fuel injector. By adding energy to this region of interest, a path for flame propagation can be created across the gap. While in operation these devices create an artificial anchor point for the flame. This allows the placement of the flame initiation site almost anywhere on the combustor walls where fuel is present.

* President, GoHYPERSONIC Inc., 714 Monument Ave., Ste 201, Dayton, OH 45402, Member AIAA.
† Senior Aerospace Engineer, AFRL/PRAS, Bldg 18, 1950 Fifth St., WPAFB, OH 45433, Associate Fellow AIAA.
‡ Senior Engineer, GoHYPERSONIC Inc., 714 Monument Ave., Ste 201, Dayton, OH 45402, Member AIAA.

As with all real estate, location proves to be a very important factor. When selecting the *ideal* location for an igniter, one must pay attention to how the igniter jet will couple to the fuel jet it is attempting to burn. In addition to the physical locations of the devices, the composition of both the fuel and the *hot* gas used as the initiator must also be well thought out; the ideal location for a hot oxidizer stream may not be the same location for an igniter that utilizes hot fuel and combustion products. Simple hot inert gas or pyrophoric agents may be more effective in alternate regions too.

Two particular upstream flush-wall cavity-coupled injectors of interest at the AFRL are the low angled 15-degree sonic hole and the aero-ramp[2,5]. Both types of fuel injectors have been studied in scramjet combustors for the injection of gaseous hydrocarbon fuels[1,6,7,8] upstream of a flameholding cavity. Of particular interest to this study are the experiments conducted by Gruber et al.[9] This study involved 15-degree cavity-coupled injectors at a slightly smaller scale with a similar dimensioned cavity and was performed in the same experimental facility as the present study. Ignition in this study was accomplished by establishing a flame first within the cavity by a co-located sparkplug. To accomplish this feat with upstream fuel injection over a wide range of fuel flow proved to be challenging. The desire for a spatially uniform fuel-air mixture to mitigate sensitivity to changes in fuel flowrate and the main-duct flow during ignition led to the incorporation of several secondary cavity fueling concepts.

In this work, tests were conducted to study the mixing and entrainment process of the above mentioned two types of cavity-coupled fuel injectors (the aero-ramp and the 15-degree injector). In addition to comparing types of injectors, gas was injected though smaller secondary holes located upstream and downstream of the main injectors to simulate a hot gas igniter – such as a plasma torch, pyrophoric effluent, or other type of igniter – just upstream of the cavity. Injection through an additional 15-degree hole, located near the sidewall of the wind tunnel duct was also examined to help discern any differences in mixing and the coupling of the simulated igniter plumes and the main jets due to their proximity to the wall. Cavity fueling was not considered for this study; instead, emphasis was placed on understanding the interaction of the fuel jets with the simulated igniter jet plumes. Both the simulated igniter and fuel injector holes injected room temperature air, respectively seeded with acetone or nitric oxide (NO). Characterization of the main-stream flow in a plane near the front of the cavity region was also performed by in-stream pressure measurements made with a set of probes in the duct, with and without backpressure (where the purpose of backpressuring the duct was to simulate the pressure rise expected with combustion). Subsequently, the jet plumes of the various injector configurations were studied using planar laser-induced fluorescence with and without backpressure.

Hardware

Tests were conducted in a Mach 1.94 crossflow. The tunnel dimensions consisted of a 2.5-degree diverging duct (start of divergence was at the upstream end of the injector-cavity floor plate) with initial test section cross-stream dimensions of 50.8 by 152.4 mm, while the layout of the injectors and torch holes is shown in Figs. 1 and 2. Nomenclature associated with the plasma torch holes at the centerline are shown in Fig. 2: C-T and S-T indicate the Central-Torch and the Side-Torch, respectively, while the numbers inside the brackets represent the streamwise and cross-stream location, respectively. This study used an injector-centered, right-hand Cartesian coordinate system with the X-axis located in the cross-stream direction, the Y-axis in the vertical direction, and the Z-axis located in the downstream direction as shown in Fig. 2. The dimensional relation of the all the various orifices and the cavity section are shown in Table 1 and Table 2. The injector diameter nomenclature $D_{1\text{-}H}$ and $D_{EQ,4\text{-}H}$ stand for the diameter and equivalent diameter of the 15-degree single-hole and aero-ramp sonic injectors, respectively. The central injector blocks were fabricated for use in Jacobsen et al[1]. The 15-degree single-hole injector located adjacent to the side wall is identical to the centrally located single counterpart and is at the same downstream location.

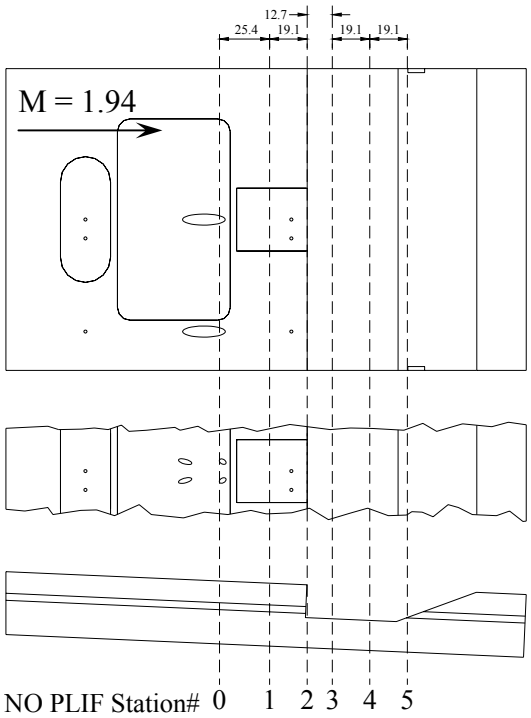

Fig. 1 Injector-cavity floor plate. Tunnel floor plate has a single-hole injector located near the sidewall and a centrally located injector insert block containing either a single-hole or an aero-ramp injector. The hole-area centers of the single-hole and aero-ramp injectors are at the same streamwise location. NO PLIF laser sheet stations and relative locations are also shown. (Dimensions in mm.)

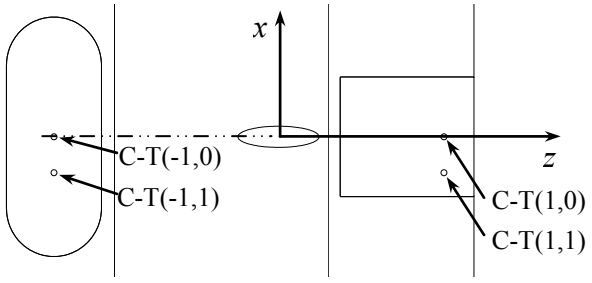

Fig. 2 Lateral simulated Central-Torch (C-T) stations relative to middle injector axial centerline. Single-hole injector insert is shown here.

Table 1 Injector-torch-cavity *streamwise* locations relative to the center of the injector. Cavity has a 22.5º ramp on the downstream end and a length to depth ratio of 4.0 (6.60 cm/1.65 cm).

	C,S-T (-1,0)	Injector	C,S-T (1,0)	Cavity L.E.	Cavity T.E.
From Injector Center (cm)	-6.01	0.00	4.43	5.23	13.83
$Z/D_{1\text{-}H}$ (5.61 mm)	-10.71	0.00	7.89	9.32	24.63
$Z/D_{EQ,4\text{-}H}$ (4.76 mm)	-12.62	0.00	9.30	10.98	29.03
From Cavity L.E. (cm)	-11.24	-5.23	-0.80	0.00	8.60
$Z/D_{1\text{-}H}$ (5.61 mm)	-20.02	-9.32	-1.43	0.00	15.31
$Z/D_{EQ,4\text{-}H}$ (4.76 mm)	-23.60	-10.98	-1.69	0.00	18.05

Table 2 Injector-torch-cavity *lateral* locations relative to middle injector axial centerline. Side-Torch (S-T) locations are on streamwise centerline of side injector (in-line) only.

	Center Inj.	Side Inj	Side Wall	C-T (±1,0)	C-T (±1,1)
From Tunnel Centerline (cm)	0.00	5.66	7.62	0.00	0.95
$X/D_{1\text{-}H}$ (5.61 mm)	0.00	10.08	13.57	0.00	1.70
$X/D_{EQ,4\text{-}H}$ (4.76 mm)	0.00	N.A.	16.00	0.00	2.00
	Center Inj.	Side Inj	Side Wall	S-T (-1,0)	S-T (1,0)
From Tunnel Side Wall (cm)	7.62	1.97	0.00	1.97	1.97
$X/D_{1\text{-}H}$ (5.61 mm)	13.57	3.50	0.00	3.50	3.50
$X/D_{EQ,4\text{-}H}$ (4.76 mm)	16.00	N.A.	0.00	N.A.	N.A.

Test Matrix

Flow Conditions

Test conditions consisted of supersonic flow with an initial Mach number at the end of the facility nozzle of 1.94. The freestream total pressure was 25 psia for all experiments. The freestream total temperature was either ambient temperature at about 290 K during the intrusive sampling and at about 590 K during the laser diagnostics experiments to minimize acetone condensation and any condensation scattering produced from the condensation of acetone. Note that to apply a high tunnel backpressure, a butterfly valve downstream of the test section was partially closed, forcing the shock train up to near nozzle exit; by this means, the pressure rise from main duct combustion could be simulated.

Table 3 shows the injector flow rates employed in the study. Also shown in the table are discharge coefficient (C_d), injector total pressure ($P_{t,j}$), and the jet-to-freestream momentum flux ratio (Qbar). The simulated plasma torch injector air flow rates were kept at 15 SLPM (Standard Liters Per Minute based on the density of air at 1 atm and 298 K) for all the experiments. All injectant gas came from bottled air kept at ambient conditions (298 K). However, NO within N_2 (from a bottle containing 10,000 ppm, parts per million in N_2) was added to the injectant air stream. The NO-doped nitrogen concentration was kept to 10% of the total flow through the injector so that the injectant was typically composed of nominally 81% N_2, 19% O_2, and 0.1% NO by volume. During the side-wall injector experiments, the NO volume fraction was reduced to 0.05% due to a shortage of gas. Acetone was introduced into air by running air through a warm bath of acetone kept at 313 K and then through a secondary chamber maintained at room temperature to keep the acetone concentration within the injectant reasonably constant (and reasonably large).

Table 3 Nominal main injector flowrate settings.

Flow Condition	Air (SLMP)	NO (SLMP)	Total (SLMP)	Total (gm/sec)	C_d	Pt,j (psia)	Qbar
Low	225	25	250	5.1	0.89	19.2	1.1
High	540	60	600	12.3	0.92	44.7	2.5

Test Series

To characterize the flow in the duct with and without applied backpressure, where the mixing process would take place during the injection studies, in-stream pressure measurements were made with a set of probes at the front of the cavity region. Subsequently, the jet plumes of the various injector configurations were studied using laser diagnostics with and without backpressure. The primary comparisons during the study were the centerline single-hole and aero-ramp injector, the influence of duct position (center to side-wall) on the injection process of the single-hole injector, and the entrainment process of the simulated plasma torch plumes into the injector jets and the cavity.

Experimental Techniques

Aerothermodynamic Sampling

In-stream Pitot and cone-static pressure measurements were made with a standard set of probes. The Pitot probe had an outer diameter of 3.18 mm and the cone-static probe had a cone half-angle of 10 degrees. Pressure measurements were made on a grid with data points spaced 0.25 cm in both horizontal and vertical cross-stream directions. The two probes were mounted on opposing walls in the cavity section of the duct. The sampling stations of each probe were limited to half of the duct and symmetry is to be assumed in the data reduction technique. The vertical sampling plane was located 0.9 cm downstream from the leading edge of the cavity.

Laser Induced Fluorescence

Two Planar Laser Induced Fluorescence (PLIF) techniques were used to visualize the jet plumes. The main injector plumes were visualized using a Nitric Oxide (NO) PLIF and the simulated plasma torch plumes were visualized using acetone PLIF. For NO PLIF the output of a Nd:YAG-pumped dye laser, operating at 574 nm, was frequency doubled to 287 nm; this radiation was then mixed with the residual 1064-nm radiation from the Nd:YAG to produce 226-nm radiation to excite the overlapped $Q_1(12.5)$ and $Q_2(20.5)$ transitions in the $A\Sigma-X\Pi$ (0,0) band. Fluorescence from the A–X (0,1), (0,2), (0,3) … bands was then detected using an intensified CCD (PI-MAX with Superblue intensifier) fitted with a Nikon UV Nikkor 105-mm focal length, f/4.5 lens; only a UG-5 Schott glass filter, which has a sharp "cut-on" edge at 230 nm, was used to block scattered laser radiation. Both the laser energy and the laser tuning were continuously monitored: a small portion of the 226-nm beam was directed over a flame and then to a photodiode. Fluorescence from the flame-generated NO was detected using a photomultiplier tube, PMT. Both photodiode and PMT signals were registered on an oscilloscope and adjustments to the laser (e.g., for laser wavelength tuning) were made as necessary. Fluorescence—and thus laser wavelength tuning—was kept relatively constant (with typical variations from one measurement to another estimated to be ±10%) by this means. For acetone PLIF the frequency-doubled output of a second Nd:YAG was again frequency doubled, using a BBO crystal. Acetone fluorescence was detected with a second PI-MAX CCD (with a blue-shifted Gen III intensifier) equipped with a Nikon 105-mm focal length, f/2.8 lens.

The gate widths on the two cameras were set at 100 ns; the lasers and their respective cameras were triggered 200 ns apart, to avoid any cross-talk. Because of this delay, the measurements are not truly simultaneous; however, in this period of time, the flow is relatively stationary. The two laser beams, at 226 and 266 nm, were combined on the same beam path. Laser-sheet forming optics consisted of a -150 mm cylindrical lens and a 1-m focal length spherical focusing lens. The positions of the 5 stations imaged during the tests relative to the leading edge of the cavity are shown in Fig. 1. Because of the spanwise probe locations, both cameras viewed the LIF off axis (i.e., the viewing axis was non-normal to the laser sheet), with the result that the images must be corrected for perspective distortion. Furthermore, this off-axis configuration results in some image blurring. For the NO measurement, this is largely mitigated with the small aperture of the UV lens and pixel binning (3x3, resulting in an effective array size of 170x170 super pixels). For the acetone LIF measurement, the larger lens aperture—with its smaller depth of field—necessitated the use of a scheimpflug mount; this sort of mount is typically used in stereoscopic particle image velocimetry, PIV, measurements and allows the camera body and the lens to be rotated independently (and for focus to be maintained off-axis imaging). The cameras were placed side by side when studying the side-wall injector and on opposite sides of the tunnel when viewing center-line injectors.

Results and Analysis

Tests were conducted to study the mixing and entrainment process of two types of cavity-coupled fuel injectors; an aero-ramp and a single 15-degree low-downstream-angled hole. In addition, the interaction of these fuel injectors with upstream and downstream holes, simulating plasma torches – or other types of hot gas plumes – was studied. Injection through a similar 15-degree hole near the side-wall was also examined to help discern any differences in mixing and the coupling of the simulated torch plumes due to the close proximity to the wall. To characterize the flow at the front of the cavity region, in-stream pressures were recorded in the duct with and without backpressure. Next, the jet plumes of the various injector configurations were studied using laser diagnostics, again with and without backpressure.

Duct Flow Characterization

The axial wall pressure distributions on the centerline of the test section floor are shown with and without applied backpressure in Fig. 3. Here, the axial wall pressure (P) is shown normalized to the isolator entrance

pressure (P_{ci}) located at the nozzle exit. Also shown at the bottom of Fig. 3 is the location of the intrusive sampling plane. Note that the maximum axial pressure rise above the cavity section during backpressure is about 3.5 times that of the baseline flow without applied backpressure. This is typical of the pressure rise levels expected in a scramjet combustor at low-to-medium fuel-to-air equivalence ratios (~0.3 – 0.5) for an isolator entrance Mach number 1.94.

Fig. 4 shows iso-contours of the local flow Mach number (M) deduced from the Pitot and cone-static pressure measurements 0.9-cm downstream from the leading edge of the cavity. At this location the duct height from the cavity floor to the ceiling was 7.44 cm. The contour plots are set up so that the boundary between the cavity and the main flow is located at Y=0 cm. The left boundary on the plots (X=0 cm) represents the tunnel centerline and the top, bottom and right boundaries represent the tunnel walls. These contour profiles show the dramatic difference between the supersonic and backpressured duct flows. It is interesting to note that the flow near the side wall is very well behaved and has a relatively small boundary layer when the flow is not backpressured (see Fig. 4a). This is due to the sudden expansion of the flow into the cavity just upstream of the probes. However, when a strong backpressure is applied to the flow, the corner region becomes significantly larger and subsonic as seen in Fig. 4b.

This strong change in backpressure – simulating before and after ignition – can have a significant affect on the penetration and mixing rate of the fuel plumes. This can lead to a potential de-coupling of the main fuel from the cavity which can cause flame blowout inside the combustor and is very injector-type and combustor-configuration dependent. For this reason secondary cavity fueling has been an important research topic at the AFRL[9].

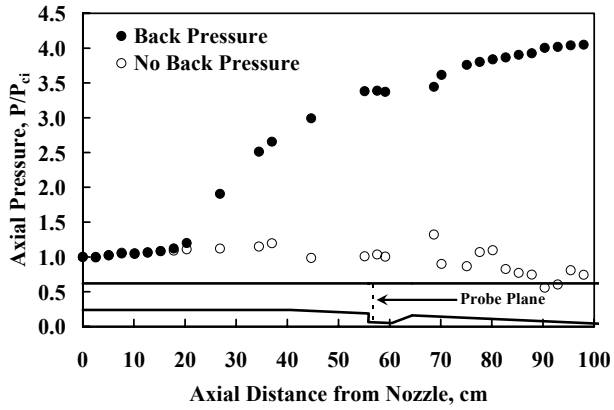

Fig. 3 Wall centerline axial static pressure measurements of test section floor with and without backpressure. Location of probe sampling plane is also shown.

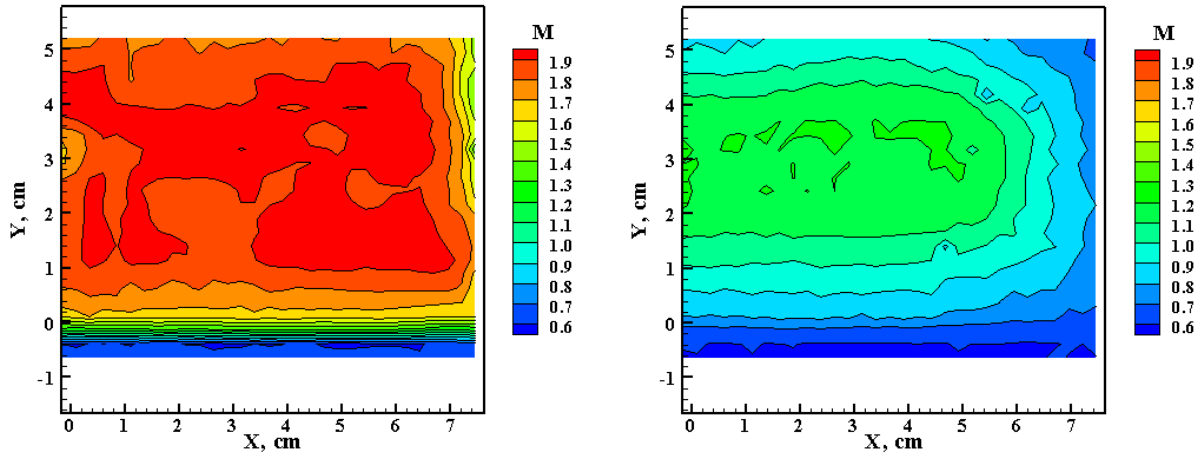

a) No backpressure. **b) Backpressure.**

Fig. 4 Mach number distribution of half wind tunnel duct deduced from Pitot and cone static probe measurements. Flow plane is 9-mm downstream of the leading edge of cavity with and without backpressure.

Injector Characterization

Fig. 5 presents the frame-averaged NO PLIF plume images of the three fuel injector plumes studied plus acetone PLIF images of the centrally located, upstream 'simulated' plasma-torch injector, C-T(-1,0). In all of the images, only one injector is being operated at a time and data is presented for sampling planes 0 – 5 from top to bottom, respectively. In the injector plume images, all three injectors are being operated at the 'high' 600 SLPM flowrate condition. The acetone injector was operated at 15 SLPM. All of the NO PLIF image intensity's (I) are normalized by the maximum intensity value (I_{MAX}) of the centrally located 15-degree injector plume at station 0. Since this plane is directly over the injector orifice, the maximum value near the surface should be comprised completely of fuel, making the intensity ratios similar to the mole fraction. This assumes that changes in the electronic quenching rate follow changes in the gas total number density and that the Boltzmann fraction of the pumped ground state and laser-transition overlap integral do not vary substantially throughout the flowfield. This assumption will be prone to some error in the near field of the injector where changes in the pressure and temperature are more substantial. No attempt was made to quantify the concentration of acetone since no data was available directly over the simulated igniter holes and the scale for these plumes is shown in Arbitrary Units, (A.U.).

The plume images for stations 0 – 2 show the region from near the center of the injector plumes right up to the leading edge of the cavity. In this region, the aero-ramp injector plume jets merge to become more-or-less one central plume. As the plumes proceed to flow over the cavity, the interaction between the injector jet and the shear layer tends to entrain the jet plumes into the cavity, as shown in varying degree by the tail-like portion at the bottom of the injector plumes.

In general, not much coupling of the injector plumes and the cavity is evident due to the relatively high flowrate of the injectors, though more entrainment of the aero-ramp plume into the cavity is evident. This portion of fuel that is entrained was already "trapped" within the boundary layer on the wall upstream of the cavity location (seen by the T-shaped plume at station 2). This could potentially provide an increased path for a flame to propagate out from the cavity flameholder as compared to the 15-degree injector plume at the same flowrate.

A plot of the NO PLIF maximum intensity ratios for the three injectors operated at the high flowrate is shown in Fig. 6. In the plot, data is shown at all six stations. Here, X=0 corresponds to the injector center or the center of the set of holes, in the case of the aero-ramp. Note that the aero-ramp data near the exit holes appears relatively low. This is because the jet exit holes near the first two sampling planes have not yet merged into a single jet and the non-dimensional spacing of the individual jets (D_j) to the sampling plane (both stations 0 and 1) is roughly 9 X/D_j, which corresponds very closely in non-dimensional distance and intensity to sampling plane 2 for the 15-degree injector. Further examination of the figure—from both the variation in relative signal strength and the plume size—also shows that the 15-degree injector on the sidewall mixed slower over the region right before the cavity and appears to increase in mixing rate thereafter, catching up to the maximum intensity ratio levels seen by the centrally located 15-degree injector on the aft ramp of the cavity. One explanation for the reduced initial mixing from the 15-degree side injector (upstream of the cavity) is that the boundary layer shape is thicker at the center than near the side walls, forming the classic '*dog-bone*' shape seen in supersonic ducts. This thicker boundary layer in the center would shield the jet more than the side mounted injector, providing a larger turbulent mixing layer for the jet. The subsequent increased mixing over the cavity near the side wall is hard to explain based on the experimental data at hand. No significant center-to-side differences were seen in the in-stream axial flow-sampling measurements near the front of the cavity which can account for this increase in mixing. However, significant axial and cross-flow vortex structures have been shown above and inside the cavity region in computational and experimental efforts with similar geometries.[6,9] These structures are created by duct-flow turning and the three-dimensional vortices inside the cavity. Differences in the mixing rate from the center to side injector over the cavity are most likely due to these types of structures.

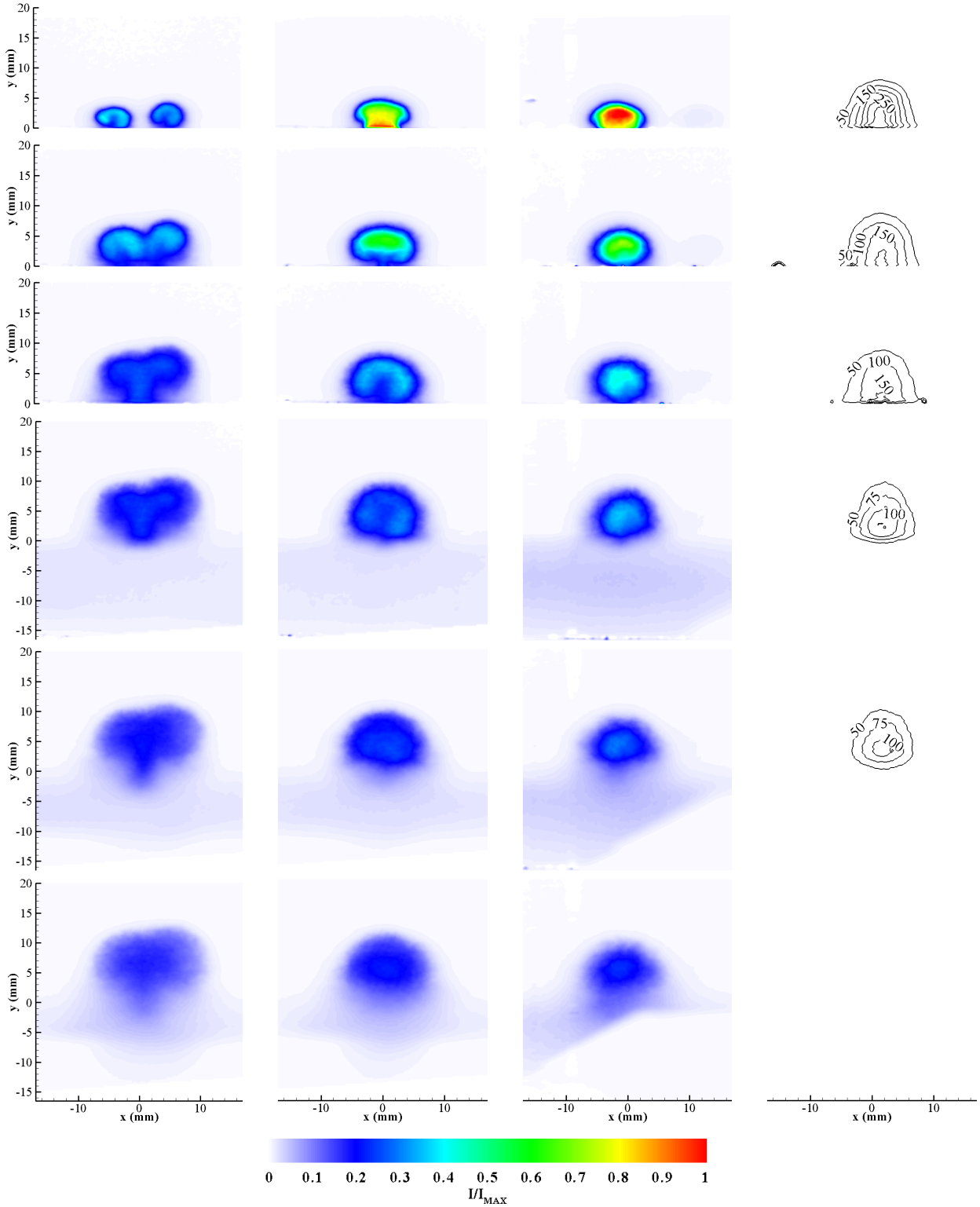

a) Aero-ramp (center). b) Single-hole (center). c) Single-hole (side). d) Simulated torch.

Fig. 5 NO PLIF seeded averaged fuel injector plumes and acetone seeded simulated plasma torch plume located at C-T(-1,0). Stations 0 – 5 are shown from top to bottom, respectively.

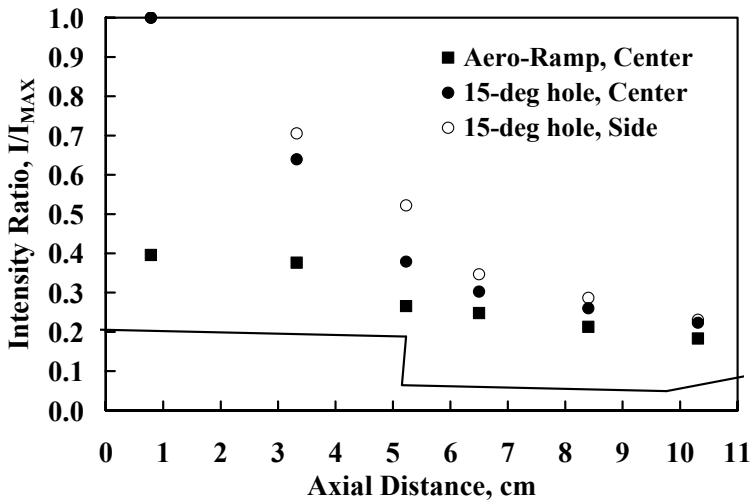

Fig. 6 Maximum intensity values of the plume cores. Wall geometry also included (vertical not to scale).

Mixing Experiments with Injectors and Simulated Igniters

Fig. 7 through Fig. 9 below show NO and acetone PLIF images at laser-sheet station 4 (see Fig. 1) of the injector and simulated igniter jet plumes. Fig. 7 shows instantaneous NO and acetone image pairs of the 15-degree injector, placed at the centerline of the wind tunnel in conjunction with the downstream in-line torch hole, C-T(1,0). This *simulated-torch* injector was located just downstream of station number 1, as shown in Fig. 1. By the time the plumes reach station 4, the two jets have significantly merged, and the simulated igniter jet has penetrated through the middle of the main injector plume to the top region of the jet. With the cavity-coupled plasma-assisted ignition concept, the plasma jet must bridge the gap between the cavity flame and the main fuel plume. If the plasma torch jet is pulled to the top of the injector plume, this may indicate that the cavity and torch-induced flames might be uncoupled in the region over the cavity, potentially making the ignition process more difficult. This would necessitate the use of higher plasma torch power to propagate a flame from the plasma jet to the region between the fuel plume and the cavity flame, versus starting with a hot plasma jet in the appropriate region.

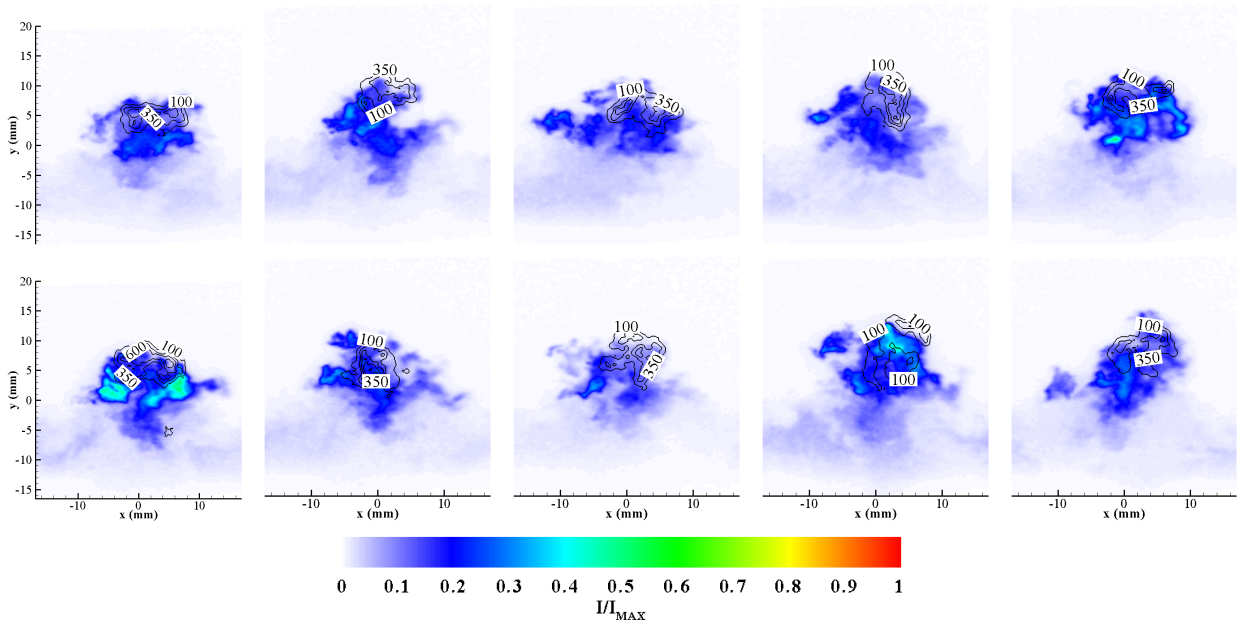

Fig. 7 Instantaneous images of center 15-degree injector at high flowrate with in-line downstream simulated plasma torch C-T(1,0) at Station 4.

Because of the desire to actively place the plasma jet into a region where it is perceived to be more effective at bridging this gap, four torch injection locations were tested; two upstream and two downstream, on and off of the centerline of both center injectors, (as shown in Fig. 1 and Fig. 2) and directly in front and behind the 15-degree side injector. In general, it is perceived that if the igniter jet were upstream of the fuel injector, it would be operated on some type of fuel. Likewise, an oxidizer-rich hot gas would be most desirable if the igniter were to be located downstream of the fuel plume.[10] Fig. 8 shows averaged plume data of the three injectors at station 4 operated at the high flowrate level run in tandem with the simulated plasma torch holes both up and downstream of the injector. At this station evidence of simulated torch plume entrainment into the cavity can be deduced for the configurations tested. If none of the simulated torch plume has entrained into the cavity by this point, it is unlikely that it will at all. This is also relevant to the issue of cavity starting, in that entrainment of the hot torch plume would be a necessity for lighting a flame inside the cavity in lieu of a cavity-based sparkplug. The results imply that the poorest configuration (of those tested) for entrainment of the igniter plume into the cavity with the aero-ramp is the location right in front of the fuel injector, while the deepest penetration of the igniter plume is achieved when it is located directly downstream of the injector. The opposite is true for the 15-degree injectors in that the igniter plume may penetrate too much when injected directly downstream of the injector. Reducing the flowrate of all the injectors tends to mitigate this entrainment deficiency as shown in Fig. 9. With both injectors studied at the tunnel centerline, placing the simulated torch plume off the injector centerline allowed good cavity entrainment at the sacrifice of injector coupling. Of these two locations some injector coupling was still accomplished with the simulated torch located downstream of the injectors C-T(1,1). Regardless of the level of injector coupling both torch locations may still be within the bridging region and still may promote flame spreading from a cavity flame to the injectors.

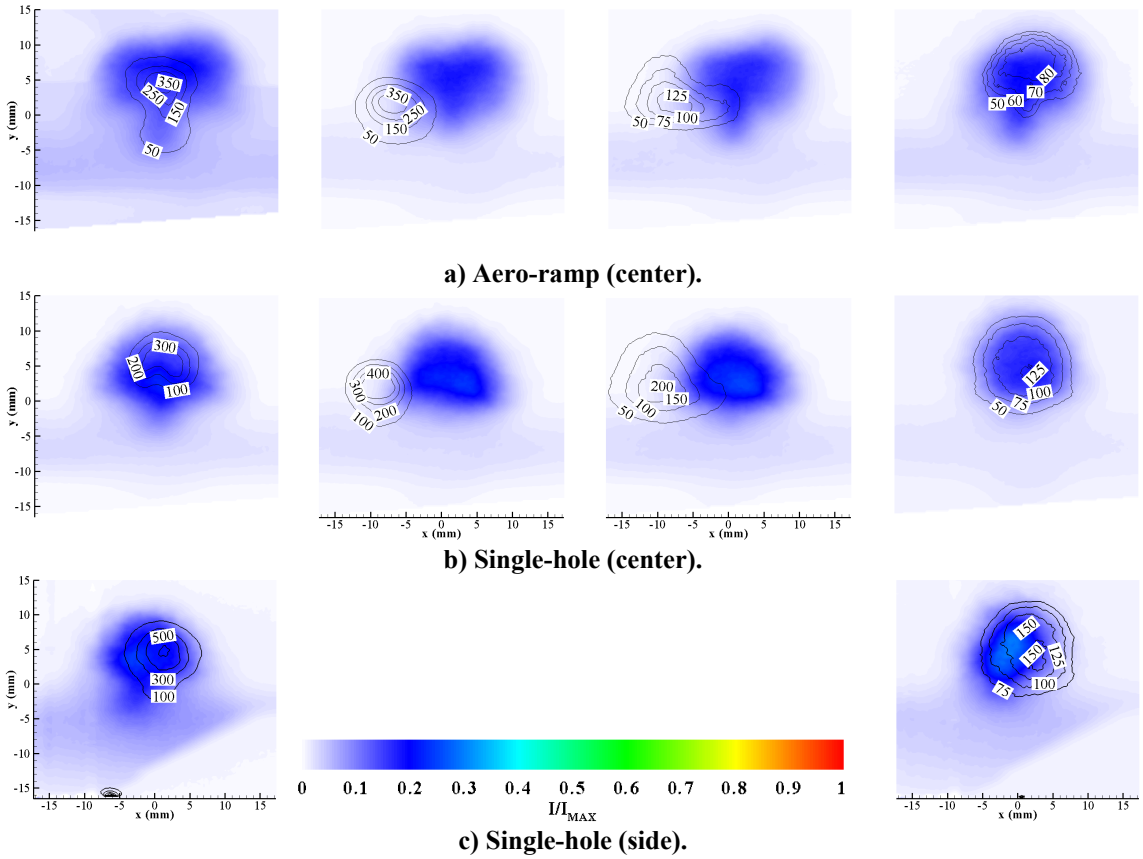

a) Aero-ramp (center).

b) Single-hole (center).

c) Single-hole (side).

Fig. 8 High flow rate, injectors with downstream in-line simulated plasma torch C,S-T(1,0) (far left), downstream off-line C-T(1,1) (left center), upstream off-line C-T(-1,1) (right center), and upstream in-line C,S-T(-1,0) (far right).

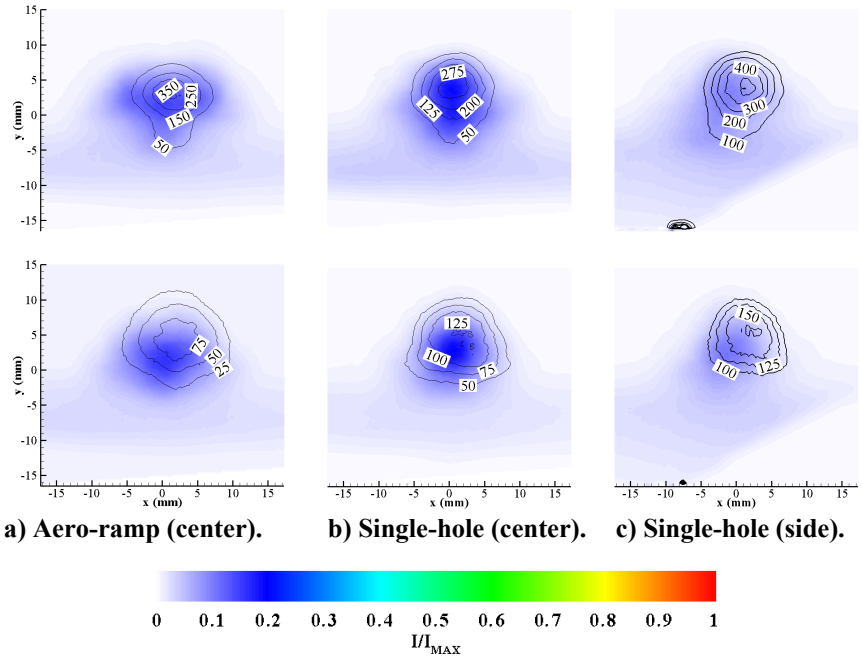

a) Aero-ramp (center). **b) Single-hole (center).** **c) Single-hole (side).**

Fig. 9 Low flow rate, injectors with downstream in-line simulated plasma torch C,S-T(1,0) (Top) and upstream center C,S-T(-1,0) (Bottom).

Data was also taken during the NO PLIF experiments with the tunnel in operation with high backpressure. As seen in the duct flow characterization section, the main-stream flow changes dramatically when the duct has been backpressured. In these experiments, the static pressure in the region of the cavity was increased to 3.5 times from the nominal levels. This new environment is shown to produce a mixed subsonic and supersonic core flow in the vicinity above the cavity, decreasing the maximum Mach number in the test section from a highly uniform ~1.9 to ~1.2 with a significant section of subsonic flow at the bottom of the duct where the fuel is being injected. Under backpressure, in the plume region of interest, the flow does not reach Mach 1 until about Y=10 mm above the duct floor (not including cavity depth) with the Mach ~1.2 core flow edge starting at about 15 mm.

Due to the facility logistics associated with keeping the test section glass clean and clear for the lasers, only a limited number of runs were possible with the tunnel operated in a backpressured mode. Data is reported here in Fig. 10 at station 2; the cavity leading edge. In this figure the NO PLIF intensity scale is once again normalized by the maximum intensity level seen directly over the center 15-degree injector hole, giving an indicator of the mole fraction of the main injector jet. Each image shows one of the three injectors studied in operation with the in-line downstream torches, C,S-T(1,0). The acetone images were not normalized and the scale for these plumes is shown in Arbitrary Units, (A.U.). These image pairs (at station 2 with and without backpressure) show the dramatic difference between the flowfield pre and post ignition. For a stable cavity flowfield during operation, the injector fuel distribution must couple well with the cavity during the transient ignition process to ensure that the cavity flameholder does not blowout as the pressure rises in the duct.

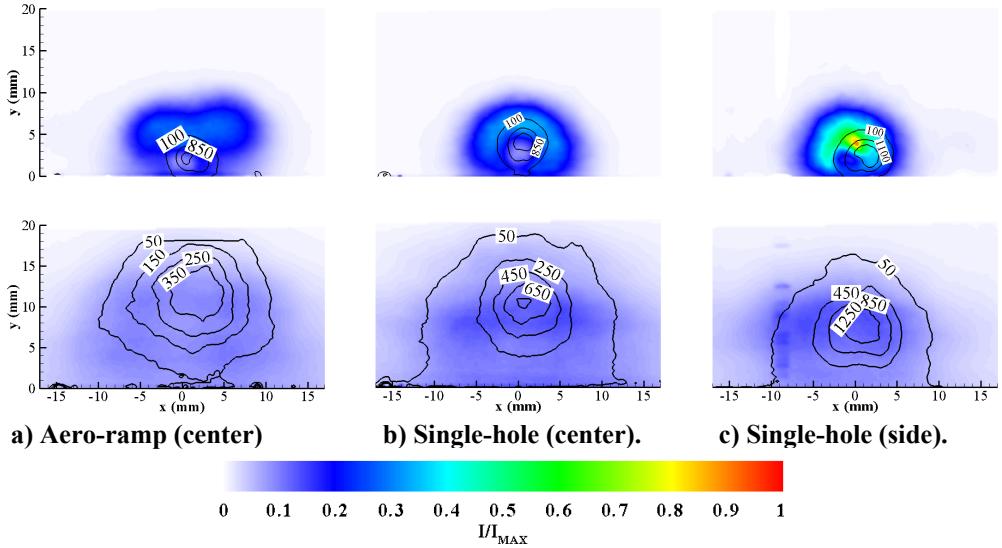

Fig. 10 High flow rate, injectors without backpressure (Upper) and with backpressure (Lower). The injectors were in operation with the downstream in-line simulated plasma torches C,S-T(1,0).

Conclusions

Tests were conducted to study the mixing and entrainment process of two types of cavity-coupled fuel injectors; an aero-ramp and a single 15-degree hole, both located upstream of a cavity flameholder. In addition, the coupling with a small normal injector – simulating a plasma jet located either upstream or downstream of the injector (and off center) – was assessed. Injection through an additional 15-degree hole, located near the side-wall of the wind tunnel duct was also examined to help discern any differences in mixing and the coupling of the simulated torch plumes due to corner effects. To characterize the flow at the front of the cavity region, where the mixing process would take place during the injection studies, in-stream pressure were recorded with a set of probes; this was done; with and without high backpressure in a effort to assess the differences in the flowfield before and after ignition has taken place (and duct combustion produces a high backpressure). Second, the jet plumes of the various injector configurations were studied using planar laser-induced fluorescence, PLIF, with and without high duct backpressure. PLIF of nitric oxide (NO) was used to track the main injectors while PLIF of acetone was used to track the tandem normal injector plumes.

Conclusions were as follows:

1. Under backpressure the static pressure in the region of the cavity was increased 3.5 times from the nominal levels. This new environment is shown to produce a mixed subsonic and supersonic core flow, decreasing the maximum Mach number in the test section from a highly uniform ~1.9 to ~1.2 with a significant section of subsonic flow at the bottom of the duct where the fuel is being injected. Under backpressure, in the plume region of interest, the flow does not reach Mach 1 until about Y=10 mm above the duct floor (not including cavity depth) with the Mach ~1.2 core flow edge starting at about 15 mm.
2. The maximum intensity ratios from the NO PLIF plumes of the aero-ramp injector were in general lower than the 15-degree injector holes. This implies that the aero-ramp injectant mixes more rapidly in the vicinity of the cavity flame holder. This increase in mixing results in an increased entrainment level into the cavity which may lead to a higher level of stability from passive upstream fueling – and/or make independent cavity fueling more difficult due to the potential for a richer environment inside the cavity flameholder.
3. The side-wall upstream 15-degree injector appears to mix more slowly (as inferred from the maximum intensity ratio and the plume size) over the region right before the cavity; eventually, by the aft ramp of the cavity, the mixing profiles for the side-wall and central 15-degree upstream injectors converge. One explanation for the reduced initial mixing deficit from the 15-degree side injector upstream of the cavity is that the overall boundary layer shape may potentially be thicker at the center and thinner just before the corners in a classic '*dog bone*' shape seen in supersonic ducts. This thicker boundary layer in the center would shield the injector more than the one on the side, providing a larger turbulent mixing layer for the jet. The subsequent increased mixing over the cavity near the side wall is hard to explain based on the

experimental data at hand. No significant center-to-side differences were seen in the in-stream axial flow-sampling measurements near the front of the cavity which can account for this increase in mixing. However, significant axial and cross-flow vortex structures have been shown above and inside the cavity region in computational and experimental efforts with similar geometries.[6,9] These structures are created by duct-flow turning and the three-dimensional vortices inside the cavity. Differences in the mixing rate from the middle to side injector over the cavity are most likely due to these types of structures.

4. The results show that entrainment of the simulated plasma torch plume into the cavity is achieved with the aero-ramp except with the igniter location right in front of the injector. The opposite is true for the 15-degree injectors in that the igniter plume may penetrate too much when injected directly downstream of the injector. Reducing the flowrate of all the injectors tends to mitigate this entrainment deficiency. With both injectors studied at the tunnel centerline, placing the simulated torch plume off the injector centerline allowed good cavity entrainment at the sacrifice of injector coupling. Of these two locations some injector coupling was still accomplished with the simulated torch located downstream of the injectors. Regardless of the level of injector coupling both torch locations may still be within the bridging region and still may promote flame spreading from a cavity flame to the injectors.

The dramatic difference between the flowfield in a scramjet pre and post ignition is considerable. For a stable cavity flowfield during operation, the injector fuel distribution must couple well with the cavity during the transient ignition process to ensure that the cavity flameholder does not blowout as the pressure rises in the duct. The placement of hot gas igniters in the vicinity of a fuel injector, both upstream of a cavity flameholder, offers a potential solution for bridging the gap between the fuel plumes and the cavity flame and maintaining a stable flame throughout the ignition process. Furthermore, cavity-coupled injector concepts must allow sufficient fuel entrainment into the cavity or couple well in steady-state operation with a cavity fueled from within. Both upstream igniter concepts, such as a combustion-based or plasma torch igniter, and secondary cavity fueling sites add additional complexity into an engine system with potential impacts at the engine performance and mission level. Therefore, they should only be added if they are required to extend the bounds of an existing simpler engine system.

Acknowledgements

This work has been supported by the Air Force Office of Scientific Research (AFOSR) and the Nunn Program Office. We would also like to thank the following people for their contributions to the effort at the AFRL: Mark Hsu, Bill Terry, and Dave Schommer of Innovative Scientific Solutions, Inc. and Robert Kielb of Pyrodyne, Inc.

References

[1] Mathur, T., Gruber, M., Jackson, K., Donbar, J., Donaldson, W., Jackson, T., and Billig, F., "Supersonic Combustion Experiments with a Cavity-Based Fuel Injector," *Journal of Propulsion and Power*, Vol. 17, No. 6, 2001, pp. 1305-1312.

[2] Jacobsen, L. S., Carter, C. D., Baurle, R. A., and Jackson, T. A. "Toward Plasma-Assisted Ignition in Scramjets," AIAA Paper 2003-0871, January 2003.

[3] Jacobsen, L. S., Carter, C. D., Jackson, T. A., Schetz, J. A., O'Brien, W. F., Elliott, G. S., Boguzko, M., and Crafton, J. W., "An Experimental Investigation of a DC Plasma-Torch Igniter," AIAA Paper 2002-5228, September 2002.

[4] Kobayashi, K., Tomioka, S., and Mitani, T., "Supersonic Flow Ignition by Plasma Torch and H2/O2 Torch," *Journal of Propulsion and Power*, Vol. 20, No. 2, 2004, pp. 294-301.

[5] Jacobsen, L. S., Gallimore, S. D., Schetz, J. A., O'Brien, W. F., and Goss, L. P., "An Improved Aerodynamic Ramp Injector in Supersonic Flow," *Journal of Propulsion and Power*, Vol. 19, No. 4, 2003, pp. 663-673.

[6] Baurle, R. A., and Eklund, D. R., "Analysis of Dual-Mode Hydrocarbon Scramjet Operation at Mach 4-6.5," *Journal of Propulsion and Power*, Vol. 18, No. 5, 2002, pp.990-1002.

[7] Gruber, M., Donbar, J., Jackson, T., Mathur, T., Eklund, D., and Billig, F., "Performance of an Aerodynamic Ramp Fuel Injector in a Scramjet Combustor," AIAA Paper 2000-3708, July 2000.

[8] Eklund, D., and Gruber, M., "Study of a Supersonic Combustor Employing an Aerodynamic Ramp Pilot Injector," AIAA Paper 99-2249, June 1999.

[9] Gruber, M. R., Donbar, J. M., Carter, C., D., and Hsu, K.-Y. "Mixing and Combustion Studies Using Cavity-Based Flameholders in a Supersonic Flow," *Journal of Propulsion and Power*, Vol. 20, No. 5, 2004, pp.769-778.

[10] Jacobsen, L. S., Gallimore, S. D., Schetz, J. A., O'Brien, W. F., "Integration of an Aeroramp Injector/Plasma Igniter for Hydrocarbon Scramjets," *Journal of Propulsion and Power*, Vol. 19, No. 2, 2003, pp.170-182.